



# Bose-Einstein transition temperature in a dilute repulsive gas

Markus Holzmann, Jean-Noël Fuchs, Gordon Baym, Jean-Paul Blaizot,  
Franck Laloë

## ► To cite this version:

Markus Holzmann, Jean-Noël Fuchs, Gordon Baym, Jean-Paul Blaizot, Franck Laloë. Bose-Einstein transition temperature in a dilute repulsive gas. *Comptes Rendus. Physique*, 2004, 5, pp.21. 10.1016/j.crhy.2004.01.003 . hal-00000770v2

**HAL Id: hal-00000770**

**<https://hal.science/hal-00000770v2>**

Submitted on 27 Nov 2003

**HAL** is a multi-disciplinary open access archive for the deposit and dissemination of scientific research documents, whether they are published or not. The documents may come from teaching and research institutions in France or abroad, or from public or private research centers.

L'archive ouverte pluridisciplinaire **HAL**, est destinée au dépôt et à la diffusion de documents scientifiques de niveau recherche, publiés ou non, émanant des établissements d'enseignement et de recherche français ou étrangers, des laboratoires publics ou privés.

# Bose-Einstein transition temperature in a dilute repulsive gas

M. Holzmann<sup>1</sup>, J.N. Fuchs<sup>2</sup>, G. Baym<sup>3</sup>, J.P. Blaizot<sup>4</sup>, and F. Laloë<sup>2</sup>

<sup>1</sup> Laboratoire de Physique Théorique des Liquides,  
UPMC, 4 place Jussieu, 75252 Paris, France

<sup>2</sup> Laboratoire Kastler Brossel, École Normale Supérieure,  
24 rue Lhomond, 75005 Paris, France

<sup>3</sup> University of Illinois at Urbana-Champaign,  
1110 W. Green St., Urbana, IL 61801, USA

<sup>4</sup> CEA-Saclay, Service de Physique Théorique, 91191 Gif-sur-Yvette, France

November 27, 2003

## Abstract

We discuss certain specific features of the calculation of the critical temperature of a dilute repulsive Bose gas. Interactions modify the critical temperature in two different ways. First, for gases in traps, temperature shifts are introduced by a change of the density profile, arising itself from a modification of the equation of state of the gas (reduced compressibility); these shifts can be calculated simply within mean field theory. Second, even in the absence of a trapping potential (homogeneous gas in a box), temperature shifts are introduced by the interactions; they arise from the correlations introduced in the gas, and thus lie inherently beyond mean field theory - in fact, their evaluation requires more elaborate, non-perturbative, calculations. One illustration of this non-perturbative character is provided by the solution of self-consistent equations, which relate together non-linearly the various energy shifts of the single particle levels  $k$ . These equations predict that repulsive interactions shift the critical temperature (at constant density) by an amount which is positive, and simply proportional to the scattering length  $a$ ; nevertheless, the numerical coefficient is difficult to compute. Physically, the increase of the temperature can be interpreted in terms of the reduced density fluctuations introduced by the repulsive interactions, which facilitate the propagation of large exchange cycles across the sample.

## Introduction

The calculation of the effects of interactions in dilute gases is often considered as a classical textbook problem, which is generally solved with the help of cluster techniques in statistical mechanics; well known examples are for instance the second virial correction to the pressure, the heat capacity, or to the magnetic susceptibility for a gas of spin 1/2 particles [1, 2]. For gases at low temperatures, all these corrections are expressed in terms of a single parameter, the scattering length  $a$ , so that the result is simple. At first sight, the calculation of the first correction to the critical Bose-Einstein condensation (BEC) temperature in a dilute repulsive Bose gas seems to raise a similar problem. Nevertheless, its solution was not well understood until recently, as illustrated by a large collection of contradictory results in the literature (see [3] and references contained). Several reasons underlie the confusion. First, for a homogeneous gas at low temperatures, it turns out that a mean field treatment of the interactions leads to an exactly zero shift of the critical temperature (the critical value of the chemical potential is shifted, but this does not affect the critical temperature); combining mean field theory with additional - and not necessarily well controlled - approximations can then lead to results which are approximation dependent, providing arbitrary  $a$  power variations and even sign. The second reason is that the problem is actually not as simple as it looks. It is essentially non-perturbative at several levels

[3, 4], even if the leading correction term which emerges from the calculations ends up being simply linear in  $a$ ; we discuss below in more detail this peculiar feature of the calculations. In retrospect, this difficulty is actually not so surprising, since the properties of a Bose gas are non-analytic around  $a = 0$ , where the system is at the border of stability (a Bose gas collapses at condensation as soon as  $a$  becomes negative). The linearity in  $a$  is therefore far from obvious, and indeed it turns out that the next correction [5] is not simply  $\sim a^2$  but  $\sim a^2 \log a$ , clearly manifesting the non-analytic character of the problem.

The purpose of the present article is to return to the considerations of [3] and [4], with more detailed discussion of some of their physical aspects. In particular, we wish to emphasize that the linearity in  $a$  of the leading term in the correction to the critical temperature may be missed if a non self-consistent theory is used to calculate the effect; indeed, some calculations found in the recent literature and based on non self-consistent models provide different results, first corrections  $\sim a \log a$  for instance. But, before we come to this point, in order to avoid any confusion, we carefully distinguish between two effects which are discussed in this context; the former takes place in traps only, the latter also in a uniform gas contained in a box.

## 1 Compressibility effects in a trap (mean field)

For a Bose gas of  $N$  atoms contained in a trap at a given temperature, Bose-Einstein condensation first sets in at the point where the density is maximum. Repulsive interactions tend to make the density more uniform, and hence will in general lower the density at this point, so that they will decrease the transition temperature with respect to an ideal gas. Several authors have studied this effect; for a review, see ref. [6] (§ V-B) and references therein. Here, for the sake of simplicity, we limit ourselves to the discussion of isotropic traps and to the thermodynamic limit<sup>1</sup>. This excludes finite size effects, which are also discussed in [6]; a finite size system does not undergo a sharp phase transition and thus the critical temperature, and its shift, depend on a somewhat arbitrary definition of the critical temperature<sup>2</sup>. In the thermodynamic limit, this arbitrary character disappears; the width of the trap becomes large so that the effects of the trapping potential may be treated within a semi-classical approximation. Around the center of the trap, one can then completely ignore the effects of the potential, and the condensation is obtained when, locally, the critical conditions are reached. This happens when the local degeneracy parameter, the product  $n(0)\lambda^3$ , is equal to the critical value of this parameter in a homogeneous system, where  $n(0)$  is the number density at the center of the trap and  $\lambda = h/\sqrt{2\pi m k_B T}$  the thermal wavelength. For an ideal gas, this value is  $\zeta_{3/2} \simeq 2.61$ .; for a non ideal gas, it is slightly shifted, see § 2. The question now is to relate  $n(0)$  to  $N$  in order to obtain its critical value as a function of the temperature, or conversely the critical temperature as a function of  $N$ .

### 1.1 Equation of state

In a gas in equilibrium, the local density of the gas adjusts locally so that the pressure gradient in the gas compensates exactly for the force exerted by the external potential. The equation of state of the gas therefore plays an essential role in the determination of the density profile in a trap. A

<sup>1</sup>The thermodynamic limit in a trap is defined as the limit where the number  $N$  of particles tends to infinity, the frequency  $\omega$  of the trap goes to zero, and the product  $N\omega^3$  remains constant.

<sup>2</sup>In an ideal gas, the number of particles in excited states  $N_e$  can not exceed a maximum value  $N_e^{\max}$ , obtained when the chemical potential is equal to the single particle ground state energy. The usual definition of the critical value  $N_c$  for the total number of particles  $N$  in a finite trap is  $N_c = N_e^{\max}$ . This convention is convenient, but remains somewhat arbitrary, since it relates the value of one physical quantity,  $N$ , to the upper limit of another physical quantity  $N_e$ . It therefore conveys the idea of  $N_e$  increasing until it reaches its absolute upper limit, and then saturating. In reality, a large number of particles has already accumulated in the ground state when  $N = N_e^{\max}$ , and  $N_e$  actually never reaches this upper limit (except in the limit  $N \rightarrow \infty$ ).

Another definition of the critical point may be obtained by plotting the number  $N_0$  of particles in the lowest state as a function of temperature (at constant  $N$ ), and taking the inflexion point to define the critical temperature. This is in a sense more physical, but still arbitrary, and this different convention leads to different values of the finite size effects.

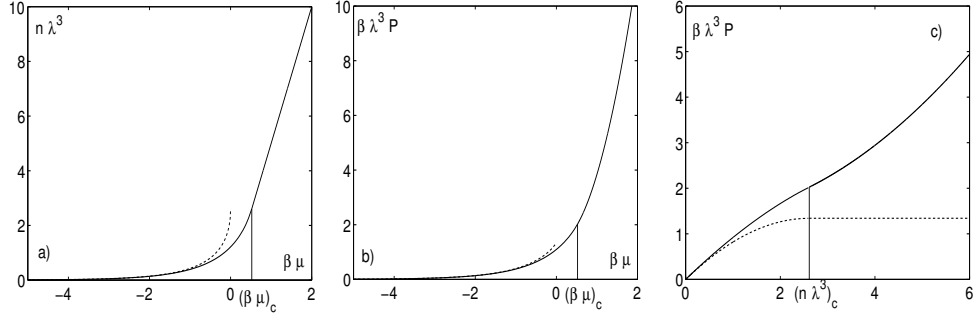


Figure 1: Figure (a) shows the number density  $n$  in the gas as a function of the chemical potential  $\mu$ , at constant temperature  $T$  ( $n$ , measured in unities of  $\lambda^{-3}$ , is dimensionless). This curve is obtained within simple mean field theory; the critical value of  $\mu$  is  $\mu_c$ ; beyond this value, the slope of the curve is inversely proportional to the scattering length  $a$ . Figure (b) shows the pressure  $P$  in the gas, which is the integral of  $n$  over  $\mu$ . Figure (c) shows the equation of state relating  $P$  to  $n$ , after elimination of  $\mu$ ; the critical value of the density is  $n_c$ ; at this point, the compressibility of the gas is proportional to  $1/a$ . Dashed lines refer to the ideal gas ( $a = 0$ ).

good approximation is provided by mean field theory, where the local density of the gas is written as:

$$n = \frac{1}{\lambda^3} g_{3/2} [z = \exp \beta(\mu - \Delta\mu)] + n_0 \quad (1)$$

with:

$$\beta\Delta\mu = 4a\lambda^2 n \quad (2)$$

where  $\beta = 1/k_B T$  is the inverse temperature,  $g_{3/2}(z)$  the usual Bose function [2] and  $n_0$  the density of condensed particles. Figure 1-a shows the variations of the density<sup>3</sup> as a function of the chemical potential  $\mu$ , assuming that the gas is repulsive ( $a > 0$ ) - see for instance figure 10 of ref. [7] for a geometrical construction of this curve. Integration over the chemical potential provides the pressure (fig. 1-b); eliminating  $\mu$  leads to the equation of state in mean field approximation (fig. 1-c). For comparison, the curves are also shown for the ideal gas ( $a = 0$ ). As expected, repulsive interactions tend to increase the pressure of the gas and to reduce its compressibility.

## 1.2 Total number of particles in a trap vs. density at the center

In a trap that is sufficiently large (thermodynamic limit), the effects of the external potential can be treated semi-classically, which allows one to extend equations (1,2) to inhomogeneous systems. We now assume that the gas is not Bose condensed and define the effective chemical potential  $\mu_{\text{eff}}$  by:

$$\mu_{\text{eff}}(\mathbf{r}) = \mu - V(\mathbf{r}) - 4a\lambda^2 n(\mathbf{r})/\beta \quad (3)$$

and find:

$$n(\mathbf{r})\lambda^3 = g_{3/2} [z = e^{\beta\mu_{\text{eff}}(\mathbf{r})}] \quad (4)$$

But equation (4) can be inverted as:

$$\mu_{\text{eff}} = \beta^{-1} J(n\lambda^3) \quad (5)$$

where  $J$  is the logarithm of the inverse function of  $g_{3/2}$ . By differentiation, one obtains:

$$\nabla\mu_{\text{eff}} = \beta^{-1}\lambda^3 J'(n\lambda^3) \nabla n \quad (6)$$

<sup>3</sup>We take this opportunity to note that fig. 2 of [3] is inaccurate: at the critical value  $\mu_c$  of the chemical potential, the curve should not have a kink, but a continuous slope.

where  $J'$  is the derivative of  $J$ . Combined with (3), this equation yields:

$$-\beta \nabla V(\mathbf{r}) = [\lambda^3 J'(n\lambda^3) + 4a\lambda^2] \nabla n(\mathbf{r}) \quad (7)$$

which relates the local variations of the potential and of the density. In general, the term in  $4a\lambda^2$  on the right side of this equation is a small correction to the term in  $J'$ , so that the relation between the two gradients depends only weakly on  $a$ . Nevertheless, in regions of space where the gas is almost condensed, the derivative  $J'$  becomes very small and, for a given  $\nabla V$ , the density gradient  $\nabla n$  becomes much larger and strongly  $a$  dependent; this phenomenon can take place at the center of the trap, as we discuss in more detail in § 3.

Equation (7) allows one to calculate  $n(\mathbf{r})$  at every point of the gas as a function of  $n(0)$  and, through an  $\mathbf{r}$  integration, of the total number of particles  $N$ . At the critical point,  $n(0)$  is fixed by the condition  $n(0)\lambda^3 = \zeta_{3/2}$  in the mean field approximation<sup>4</sup>, so that this calculation provides a relation between the critical values of  $N$  and  $T$ . For a harmonic trap, where the size of the single particle ground state is  $a_{ho} = \sqrt{\hbar/m\omega}$ , Giorgini et al. [8] show that, to lowest order, this critical temperature is shifted with respect to its ideal gas value  $T_c^0$  by an amount  $\delta T_c$  given by:

$$\frac{\delta T_c}{T_c^0} = -1.3 \frac{a}{a_{ho}} N^{1/6} \quad (8)$$

Since  $N^{1/6}/a_{ho} \sim (N\omega^3)^{1/6}$ , the relative change of temperature remains finite in the thermodynamic limit. Significant critical temperature shifts can indeed be observed experimentally; for instance, recent experiments by Gerbier et al. [9] have reported observations of relative shifts as large as 10% in a Rb gas, in good agreement with (8); early Monte Carlo calculations on a trapped Bose gas also predicted a temperature shift dominated by the mean field [10] [11].

A few remarks may be useful at this stage:

(i) the shift  $\delta T_c$  describes the case where the total number of atoms  $N$  is kept constant; if, instead, the density of the gas at the center of the trap were kept constant, the shift would vanish (within mean field theory). Within a factor,  $N$  and  $n(0)$  are conjugate variables<sup>5</sup>, the former extensive, the latter intensive, somewhat similar to energy and temperature in thermodynamics. Neither of them is measured directly in experiments, since optical measurements provide the “column density” (density integrated along the line of sight), an intermediate physical quantity. Conceptually, there is nevertheless a preference for using  $n(0)$  as the relevant variable: while the calculation of the shift  $\delta T_c$  at constant  $N$  gives different results for all possible forms of traps (parabolic, quartic, or even more complicated as that shown schematically in figure 2), in the thermodynamic limit, all lead to the same value of  $n(0)$ ; this result is clearly more universal.

(ii) the physics involved in  $\delta T_c$  is only remotely related to the physics of the Bose-Einstein transition; it is more closely associated with the effects of interactions on the density profile in trap, which is in turn determined by the equation of state. In other words, the calculation of  $N$  involves many atoms which play actually no role in the condensation, because they are in regions of space where the density is too low, almost or completely in a classical regime. This is particularly obvious for the trap of figure 2 where, clearly, all the atoms in the external part of the trap are counted in  $N$ , with a weight proportional to the volume of this part, while they play no role whatsoever in the condensation phenomenon.

## 2 Correlation effects in a uniform gas

We now come to the central part of this article and discuss another shift of the critical temperature of totally different physical origin. This effect is not related to an external trapping potential but

<sup>4</sup>In all this article, we assume that the interactions can be described by a single parameter  $a$ , and therefore have no  $\mathbf{k}$  dependence. In this case, one can easily show [4][7] that, within mean field approximation, the critical value of the degeneracy parameter is unaffected by the interactions.

<sup>5</sup>When the potential is treated semi-classically, one can show that  $N = g'_{3/2}(z) \times n(0) \partial \text{Log} Z / \partial n(0)$  where  $Z$  is the partition function with the usual notation  $z = \exp \beta \mu$ .

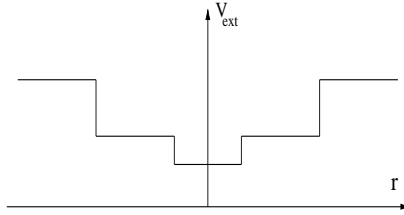


Figure 2: Example of a shape of a trap where only the central part plays a role in Bose-Einstein condensation; all the atoms in the other part are counted in the total number of particles  $N$  but do not take part in the phenomenon.

emerges from correlations between the particles; it is actually most conveniently calculated for a uniform gas contained in a box. As recalled in the introduction, the study of this shift has a long history of contradictory results, predicting either an increase or a decrease of the critical temperature, as well as variations with different powers of  $a$  (see [3]). It is now understood that correlation effects taking place in the non condensed gas just above transition lead to an increase of the critical temperature  $T_c$ , which is proportional to  $a$  in leading order:

$$\frac{\Delta T_c}{T_c^0} \simeq c a n^{1/3} \quad (9)$$

where  $c$  is a numerical positive coefficient. In [3, 4], linearity emerges as an exact result from a scaling analysis of the complete perturbation series.

In this text, we give another version of the argument leading to this linearity, with more emphasis on simple properties of non-linear self-consistent equations, and on the physical mechanism they contain. Behind the increase of  $T_c$  is a modification of the effective energies that determine the populations of the particles with low momenta. Within the framework of the non-linear self-consistent equations introduced in [7, 3, 4], and without elaborate calculations, we summarize the basic ideas that lead to the shift of the transition temperature, and comment on various points involved.

## 2.1 Non-linear equation for the single particle energy

In a non condensed gas, the diagonal elements  $\rho_k$  of the single particle density matrix can be written as:

$$\rho_{\mathbf{k}} = \left[ e^{\beta(e_{\mathbf{k}} - \mu + \Sigma_{\mathbf{k}})} - 1 \right]^{-1} \quad (10)$$

where  $\beta$  is the inverse temperature,  $\mu$  the chemical potential and the effective energy is the sum of the free particle kinetic energy  $e_{\mathbf{k}} = \hbar^2 \mathbf{k}^2 / 2m$  and the energy shift  $\Sigma_k$  introduced by the interactions. As in [7], we write<sup>6</sup>:

$$\beta \Sigma_{\mathbf{k}} = 4a\lambda^2 n - 8 \left( \frac{a}{\lambda} \right)^2 \left( \frac{\lambda}{2\pi} \right)^6 \int d^3 k' \rho_{\mathbf{k}'} \int d^3 q \rho_{\mathbf{k}+\mathbf{q}} \rho_{\mathbf{k}'-\mathbf{q}} \quad (11)$$

This equation is not exact, but a self-consistent “one bubble approximation” to  $\Sigma_{\mathbf{k}}$ ; it nevertheless allows a qualitative discussion of the properties of the more general theory and provides a

<sup>6</sup>In Ursell theory, equations (10) and (11) are naturally obtained in a self consistent second order approximation. Note that the energy shifts  $\Sigma_{\mathbf{k}}$  are then distinct from the self energies defined in Green’s function theory; in particular, they provide no information on the evolution of the quasiparticles, but just the static populations  $\rho_{\mathbf{k}}$ . See ref. [12] for a discussion of the appearance of exponentials  $\exp \beta \Sigma_{\mathbf{k}}$  in Ursell operator theory.

In Green’s function formalism, equations (10) and (11) can also be obtained with the help of additional approximations. For instance, one can neglect of the Matsubara frequency dependence of the self energies, which allows one to reconstruct in  $\rho_{\mathbf{k}}$  the Bose-Einstein distribution function appearing in (10), and recover the same equations.

reasonable estimate of the leading correction for  $\Delta T_c$  in the homogeneous system. The first term on the right side of (11) is simply the mean field term; in the low temperature regime where the interactions are described in terms of the scattering length  $a$  only, it depends only on the density:

$$n = \int \frac{d^3k}{(2\pi)^3} \rho_{\mathbf{k}} \quad (12)$$

Because this mean field is independent of  $\mathbf{k}$ , it has no effect whatsoever on the critical density (at a given temperature). The second term is more interesting; it corresponds to the effect of correlations due to interactions in the gas, and introduces a  $\mathbf{k}$  dependence of the energy shift  $\Sigma_{\mathbf{k}}$ . We will see that this shift tends to “harden” the free particle spectrum around  $\mathbf{k} = 0$ .

The condition for Bose-Einstein condensation reads:

$$\mu = \Sigma_0 \quad (13)$$

so that, in terms of the “spectrum” at the critical point:

$$W(\mathbf{k}) = \beta [e_{\mathbf{k}} + \Sigma_{\mathbf{k}} - \Sigma_0] \quad (14)$$

eqs (10) and (11) provide the following self-consistent equation:

$$W(\mathbf{k}) = \beta e_{\mathbf{k}} - 8 \left( \frac{a}{\lambda} \right)^2 \left( \frac{\lambda}{2\pi} \right)^6 \int d^3k' \int d^3q \frac{1}{e^{W(\mathbf{k}')} - 1} \frac{1}{e^{W(\mathbf{k}' - \mathbf{q})} - 1} \left[ \frac{1}{e^{W(\mathbf{k} + \mathbf{q})} - 1} - \frac{1}{e^{W(\mathbf{q})} - 1} \right] \quad (15)$$

From the spectrum we can obtain the populations  $\rho_{\mathbf{k}}$  and the critical density  $n_c$ . Actually, what we wish to obtain is the change  $\Delta n_c$  of the critical density (at constant temperature) with respect to the ideal gas value  $n_c^0 = \zeta_{3/2} \lambda^{-3}$ . We assume that only small values of  $\mathbf{k}$  contribute to this change (we discuss why this is true below); since  $W(\mathbf{k} = \mathbf{0})$  vanishes, we can replace  $[\exp W(\mathbf{k}) - 1]^{-1}$  by  $1/W(\mathbf{k})$  to obtain:

$$\Delta n_c \simeq \int \frac{d^3k}{(2\pi)^3} \left[ \frac{\beta e_{\mathbf{k}} - W(\mathbf{k})}{\beta e_{\mathbf{k}} W(\mathbf{k})} \right] \quad (16)$$

to leading order. Note that, as mentioned above, the mean-field term does not enter the problem anymore, and therefore does not influence the critical density or temperature.

At this point, it is easy to convert the change of density (16) at constant temperature into a change of temperature at constant density. The critical condition in the presence of interactions can be written as:

$$n\lambda^3 = \frac{nh^3}{(2\pi mk_B T)^{3/2}} = \zeta_{3/2} + \lambda^3 \Delta n_c(a, T) \quad (17)$$

where  $\Delta n_c(a, T)$  is given by (16). Equation (17) defines the new critical line in the temperature-density plane (fig. 3). Any point on the initial critical line (ideal gas) can be moved by a first order change of either the density, or the temperature, and reach a point on the new critical line; the only condition is that the change of the product  $n\lambda^3$  should be equal to  $\lambda^3 \Delta n_c(a, T)$  to first order<sup>7</sup>. But the same change of  $n\lambda^3$  can be obtained, either when  $\Delta n = 0$  with a change of temperature  $\Delta T$ , or when  $\Delta T = 0$  with a change of density  $\Delta n$ . In fact, for any motion in the temperature-density plane, the relative variation of the left side of (17) is given by:

$$\frac{\Delta(n\lambda^3)}{(n\lambda^3)} = \frac{\Delta n}{n} - \frac{3}{2} \frac{\Delta T}{T} \quad (18)$$

The same relative variation can therefore be obtained, either with a relative change  $\Delta n/n$  at constant  $T$ , or with a relative change  $\Delta T/T$  at constant density, provided the ratio between the

<sup>7</sup>To first order, we can ignore the difference between  $\Delta n_c(a, T + \Delta T)$  and  $\Delta n_c(a, T)$ .

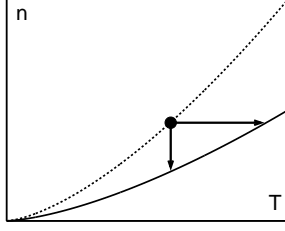


Figure 3: Critical line in the density-temperature plane, for the ideal gas (upper line) and for the interacting gas (lower line). Starting from a point on the first critical line, arrows indicate how a change of density at constant temperature, or conversely, move the point to the new line, as discussed in the text.

two changes is  $-2/3$ . Finally, the leading term of the change of critical temperature  $\Delta T_c$  is given by:

$$\frac{\Delta T_c}{T_c^0} \simeq -\frac{2}{3n_c^0} \int \frac{d^3k}{(2\pi)^3} \left[ \frac{\beta e_{\mathbf{k}} - W(\mathbf{k})}{\beta e_{\mathbf{k}} W(\mathbf{k})} \right] \quad (19)$$

We will see in § 2.1.2 that the change of the spectrum at the critical point manifests itself primarily in a small  $k$  region centered at the origin and of width  $\Delta k$  given by:

$$\Delta k = k_c \sim \frac{a}{\lambda^2} \quad (20)$$

In this region, the correction  $\Sigma_{\mathbf{k}} - \Sigma_0$  is comparable to the free particle energy  $e_{\mathbf{k}}$ , or may even dominate in  $W(\mathbf{k})$ ; this property is also discussed in detail in [3, 4]. The physical origin of the change of energy is simple: the atoms with very low velocities are extremely sensitive to even very small effects of the interaction potential. They can therefore rearrange themselves in space to minimize their repulsive energy, reaching a smaller value than the mean field prediction. On the other hand, the atoms with higher  $k$  values than  $\Delta k$  have too much kinetic energy to do so.

This rearranging process can be regarded as an analogue, in terms of interaction potential and correlations, of the effect of a weak external potential on particle positions discussed by Lamb et al. [13]. These authors point out that the character of the Bose-Einstein condensation is qualitatively modified even by a weak external potential, transferring it from momentum space to real space. Here we have another illustration of the extreme sensitivity of a gas just above transition to any potential, but in the space of relative positions instead of ordinary position of the particles.

### 2.1.1 Non self-consistent approximation: spurious logarithms

The non-linear equations (10,11), or (15), are not easy to solve. One can start by assuming that  $\Sigma_{\mathbf{k}}$  provides only a small correction to the free particle spectrum, so that the right side of (11) can be calculated with  $\Sigma_{\mathbf{k}} = 0$ , which provides a first approximation for  $\Sigma_{\mathbf{k}}$  - this operation can be regarded as a first iteration of an infinite process leading to a fully self-consistent solution. The critical condition (13) then gives an implicit equation in  $\mu$  to determine the critical value of the chemical potential (still within this first iteration). For this value of  $\mu$ , one can then use (10) to calculate the new populations  $\rho_{\mathbf{k}}$ , and finally  $n$  by integration over  $k$ . This is precisely what was done in [7] for values of  $a/\lambda$  ranging from  $10^{-3}$  to  $10^{-2}$ , leading to the following value of the coefficient  $c$  (obtained by dividing the relative change of  $T_c$  by  $an^{1/3}$ ):

$$c \simeq 0.7 \quad (21)$$

One can of course also make two (or more) iterations: again choose  $\mu$ , calculate the first approximation for  $\Sigma_{\mathbf{k}}$ , the first approximation for  $\rho_{\mathbf{k}}$ , inject them into (11) to obtain the second approximation for  $\Sigma_{\mathbf{k}}$ , and then only determine  $\mu$  by the condensation condition. The second



approximation for  $\rho_{\mathbf{k}}$  eventually provides the critical density by integration over  $k$ . This procedure leads to a progressive hardening of the spectrum, as illustrated by Fig. 15 of [7], and typically to higher values of  $c$  than suggested by the first iteration approximation, eq. (21).

But what is the validity of these calculations? Knowing that the presently accepted value is  $c \simeq 1.3$  [14, 15], at first sight one could consider this calculation a success, especially in view of its simplicity. However, success may be pure coincidence! In fact, an analytical study of the single iteration procedure shows that it does not lead to a linear dependence of  $\Delta T_c$  in  $a$ , but actually contains spurious logarithms in  $a$ ; these logarithms will dominate in the limit  $a \rightarrow 0$  and destroy the linearity - we come back to this point in § 2.2.1, but see also § 5.1 of [3]. In other words, if the numerical calculations leading to (21) had been made with a different range for the parameter  $a/\lambda$ , a different value for the coefficient  $c$  would have been obtained, as illustrated by the table of § 5.1 in [3]. The validity of the first iteration leading to eq. (21) is therefore difficult to assess a priori; see [16] for another example of a calculation which predicts a non-linear leading correction, an  $a \log a$  in this particular case.

### 2.1.2 Self-consistent treatment: linearity

We now come back to the full equation (15) and discuss the properties of the self-consistent solution  $W(\mathbf{k})$ . We define the dimensionless function  $v(x)$  of the dimensionless variable  $x = k\lambda^2/a$  by:

$$W(\mathbf{k}) = \frac{a^2}{\lambda^2} v\left(\frac{k\lambda^2}{a}\right) \quad (22)$$

Inserting this into (15) provides:

$$\begin{aligned} v(x) = & \frac{x^2}{4\pi} - \frac{8}{(2\pi)^6} \int d^3x' \int d^3y \frac{(a/\lambda)^2}{e^{(a/\lambda)^2 v(\mathbf{x}')} - 1} \frac{(a/\lambda)^2}{e^{(a/\lambda)^2 v(\mathbf{x}' - \mathbf{y})} - 1} \times \\ & \times \left[ \frac{(a/\lambda)^2}{e^{(a/\lambda)^2 v(\mathbf{x} + \mathbf{y})} - 1} - \frac{(a/\lambda)^2}{e^{(a/\lambda)^2 v(\mathbf{y})} - 1} \right] \end{aligned} \quad (23)$$

If we take the limit  $a/\lambda \rightarrow 0$  of the integrand on the right side of this equation (an operation justified below), we obtain the parameter-free self-consistent equation:

$$v(x) = \frac{x^2}{4\pi} - \frac{8}{(2\pi)^6} \int d^3x' \int d^3y \frac{1}{v(\mathbf{x}')v(\mathbf{x}' - \mathbf{y})} \left[ \frac{1}{v(\mathbf{x} + \mathbf{y})} - \frac{1}{v(\mathbf{y})} \right] \quad (24)$$

(one can easily check that no other choice for the powers of  $a$  and  $\lambda$  in the scaling factors of (22) would allow the same complete disappearance of all parameters from the equation).

We now assume<sup>8</sup> the existence of a solution to (24) that, for values of  $x \gg 1$ , is dominated by the free spectrum term  $x^2/4\pi$ . We note that the integral is made ultraviolet (UV) convergent by the difference that appears in the brackets. As for infrared (IR) convergence, for small  $x$ 's the self-consistent solution will automatically have a harder variation than  $x^2$  (free spectrum) in order to make the integral convergent, a variation in  $x^{3/2}$  for instance<sup>9</sup> [17]. Being convergent, the value of the integral can be obtained with arbitrary accuracy from a finite domain of the dimensionless variable  $x$ , corresponding to  $|x| < D$  (where  $D$  is a pure number). Coming back to (23), we see that the exponent in the denominator is smaller or equal to  $(a/\lambda)^2 v(D)$ , which tends to zero when  $a/\lambda \rightarrow 0$  (since  $v(D)$  is a pure number, independent of  $a$ ). This, in retrospect, justifies the lowest order expansion of the exponentials inside the integrand which led us to (24), at least for values of the current variable  $x$  which are not too large (see below).

Finally, inserting (22) into (16) provides:

$$\Delta n_c = -\frac{2}{\pi\lambda^2} \int dk \frac{(a/\lambda)^2 v(k\lambda^2/a) - (k\lambda)^2/4\pi}{(a/\lambda)^2 v(k\lambda^2/a)} \quad (25)$$

<sup>8</sup>This assumption is supported by numerical and analytical calculations of [3].

<sup>9</sup>A simple power counting argument applied to equation (24) predicts a  $x^{3/2}$  dependence of  $v(x)$  for small values of  $x$ .

or, with a variable change  $x = k\lambda^2/a$ :

$$\Delta n_c = -\frac{2a}{\pi\lambda^4} \int dx \frac{v(x) - x^2/4\pi}{v(x)} \quad (26)$$

This result is equivalent to (16) and shows that the density shift at constant temperature is indeed linear in  $a$ ; consequently, the same property is true for the temperature shift at constant density.

The values of the dimensionless variable  $x$  that contribute to the integral are smaller or comparable to  $D$ . In terms of the initial momentum variables appearing in (15), this domain has a range given by some number multiplying  $k_c$  defined in (20). Going from (23) to (24) actually also requires that the current variable  $x$  not be too large, namely that  $v(x) \ll (\lambda/a)^2$ . Since, for large  $x$ ,  $v(x)$  is dominated by the kinetic energy term  $\sim x^2$ , this condition corresponds to  $x \ll \lambda/a$  and therefore to  $k\lambda \ll 1$ . In other words, the values of  $\Sigma_{\mathbf{k}}$  obtained from (24) are correct, but only for momenta significantly smaller than the maximum thermal momentum. This caveat is irrelevant for the calculation of the leading term of the density shift. As we will see in more detail in § 2.3.1, what is important is the crossover value of  $k$  at which the function  $v(x)$  switches from a behavior dominated by the integral to a behavior dominated by the quadratic kinetic energy. From (24), we know that this phenomenon takes place for some finite value of  $x$  which corresponds, in terms of  $k$ , to a multiple of  $k_c$ . Finally, it is easy to see in (20) that, for sufficiently small values of  $a$ , the product  $k_c\lambda$  remains much smaller than 1, which means that only particles with low momentum have a role in the change of critical density.

The conclusion is that the non-linear self-consistent equation for the effective energies leads to linear  $a$  dependences of the temperature shift, but only if it is treated self-consistently; otherwise, more complicated spurious variations are introduced - see also ref. [18] for other numerical illustrations of this property.

## 2.2 Generalization

We now go beyond the simple approximation (11) for the effective energy and generalize the considerations of the preceding section. In the complete theory [3, 4], the right side of this equation contains an infinite sum of integrals, corresponding to all diagrams in the theory. They start from the second order term in  $a/\lambda$  already contained in (11), and continue with terms of all orders in  $a/\lambda$ , containing higher dimensional integrals with more elaborate structure. The problem then becomes significantly more complicated; we will see, nevertheless, that most of the conclusions of the preceding section remain valid. We first discuss the general relation between infrared convergence of the theory and the linearity in  $a$  of the leading term in the correction, then show that the linearity of the simple model remains valid within the general theory, and finally emphasize the difficulties arising in the precise calculation of the linear coefficient  $c$ .

### 2.2.1 Linearity and infrared convergence

It is well known that the perturbative treatment of second order phase transitions gives rise to infrared (IR) divergences. Here, we discuss the close relation between these divergences and a possible breakdown of the linearity in  $a$  of the critical temperature shift.

Let us first come back to the single iteration approximation discussed in § 2.1.1. If we introduce again the effective chemical potential  $\mu_{\text{eff}} = \mu - 4a\lambda^2 n/\beta$ , we see that this approximation involves integrals - right side of (11) - which, because they contain the ideal gas spectrum  $e_{\mathbf{k}} \sim k^2$ , are IR divergent if  $\mu_{\text{eff}} = 0$ . More precisely, when  $\mu_{\text{eff}} \rightarrow 0$ , one obtains  $\beta\Sigma_0 - 4a\lambda^2 n \sim (a/\lambda)^2 \log(-\beta\mu_{\text{eff}})$ , so that the critical condition (13) leads to logarithms in the value of the critical chemical potential,  $-\beta\mu_{\text{eff}}^c \sim (a/\lambda)^2 \log(\lambda/a)$ . But, for small  $k$ , the integrand can be written as:

$$[\beta(e_{\mathbf{k}} - \mu_{\text{eff}})]^{-1} = \beta^{-1} [(\hbar^2 k^2/2m) - \mu_{\text{eff}}]^{-1} \sim [(k\zeta)^2 + 1]^{-1} \quad (27)$$

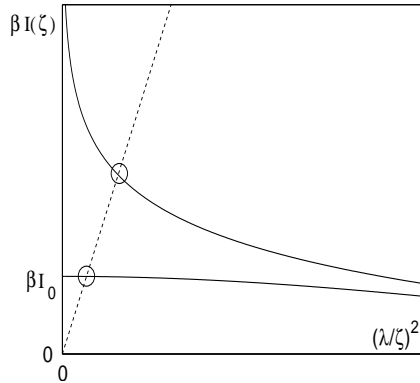


Figure 4: Graphical construction to obtain the mean field correlation length,  $\zeta$ ; the lowest full line corresponds to the absence of IR divergences, the upper full line to an IR diverging function. The slope of the dashed line is proportional to  $(\lambda/a)^2$  and diverges in the limit  $a \rightarrow 0$ .

where the mean field correlation length  $\zeta$  is defined by  $-\mu_{\text{eff}} = \hbar^2/2m\zeta^2$ , as in refs. [3, 4]. We then see that  $\zeta$  plays the role of a scaling factor for the  $k$  dependence of the energies:

$$W(\mathbf{k}) \sim \frac{a^2}{\lambda^2} v(k\zeta), \quad (28)$$

where  $v(x)$  is a dimensionless function. We can finally use this result to calculate the critical density shift, eq. (16), and obtain  $\Delta n_c \propto \zeta^{-1}$ , which is proportional to  $(a/\lambda^2)\sqrt{\log(\lambda/a)}$ .

For extremely small values of  $a$ , the logarithmic dependence on  $a$  of the correlation length then dominates the shift of the critical temperature. This explains why the table of [3] gives values of  $c$  that depend slightly on the ratio  $a/\lambda$ . Nevertheless, this logarithmic scaling is spurious, an artifact of the truncation of the self-consistent equations at the first iteration; as we have seen in § 2.1.2, the complete self-consistent solution leads to a shift of  $T_c$  linear in  $a$ .

More generally, the relation between IR convergence and linearity is easy to understand. The critical condition (13) is the key to the calculation of the scaling factor  $\zeta_c$  at the critical point, which in turn determines the critical density. Since  $\Sigma_0$  can be written as:

$$\Sigma_0 = \frac{4a\lambda^2 n}{\beta} - \left(\frac{a}{\lambda}\right)^2 I(\zeta) \quad (29)$$

where  $I(\zeta)$  is a positive integral depending on the chemical potential through  $\zeta$ , the critical condition (13) reads:

$$-\mu_{\text{eff}} = \frac{\lambda^2}{4\pi\beta\zeta^2} = \left(\frac{a}{\lambda}\right)^2 I(\zeta) \quad (30)$$

Graphically, as shown in figure 4, the critical value of  $\zeta^{-2}$  is obtained by intersecting a straight line with large slope  $(\lambda/a)^2$  with the function  $I$ , considered as a function of  $\zeta^{-2}$ . The intersection point is close to the vertical axis. If  $I$  has a finite limit  $I_0$  when  $\zeta^{-2} \rightarrow 0$ , we immediately obtain  $\zeta^{-2} \sim \beta I_0 a^2/\lambda^4$ , and from this simple scaling factor linearity in  $a$  follows. On the other hand, if this function diverges when  $\zeta^{-2} \rightarrow 0$ , the scaling factor has a more complicated  $a$  dependence.

Ref. [3] discusses various models illustrating the relation between the absence of IR divergences and the linearity in  $a$  of the leading term in the correction. For instance, the “bubble sum”, or the “ladder sum”, both contain integrands with fractions that automatically control the divergences, and therefore lead to linear dependences of the density shift in  $a$ . This property explains why ref. [19] predicts a linear  $a$  dependence, in an approach based on the many body  $T$  matrix approximation, similar to a ladder sum approximation. Clearly, these results do not establish the linearity in  $a$  for the full theory, since there is no special reason why only bubbles or ladder should be retained

from the full series. The disappearance of the IR divergences from the bubble or ladder sums is a special property of these subseries. For the reasons discussed above, one could expect the density corrections to be dominated by other diagrams containing IR divergences, therefore providing a result in  $a \ln a$  for instance (this is indeed the result obtained later in ref. [16]), and making the contribution of isolated ladders negligible. We now discuss the full theory to examine why the linearity in  $a$  is actually preserved.

### 2.2.2 Linearity in the full theory

The reasoning of § 2.1.2 can be extended to the more complicated structure of the effective energies in the complete theory. We refer the reader to the discussion given in § 4 of ref. [3]; here, we give only a brief discussion of the argument leading to linearity. The various terms in  $\Sigma_{\mathbf{k}}$ , corresponding to a series of diagrams with increasing powers of  $a/\lambda$ , may be obtained by recurrence from one order to the next. At each step, one includes one more power of  $a/\lambda$ , one more  $\mathbf{k}$  integral with a factor  $\lambda^3$ , and two more  $\rho_{\mathbf{k}}$ 's, introducing two fractions with exponentials of  $W(\mathbf{k})$  in the denominator. Now, if we make the same change of variable  $x = k\lambda^2/a$  as before, we see that the change of integration variable introduces an additional factor  $(a/\lambda^2)^3$ , which comes in addition to an  $a/\lambda^2$  from the two coefficients above; altogether, we get precisely the factor  $(a/\lambda^2)^4$  that is necessary to add a factor  $(a/\lambda^2)^2$  to the numerator of each fraction, exactly as in (23). As a consequence, we obtain again a parameter free non-linear equation, generalizing (24).

This new integral is more ultraviolet convergent than in the right side of (24) since, for large  $x$ , two additional factors of  $x^2$  overcompensate the additional integration factor  $d^3x$ . As for IR convergence, again it is obtained because the solution  $v(x)$  has to adapt its small  $x$  behavior to ensure it. Finally, the reasoning of § 2.1.2 can be made again with the more complicated non-linear equation, so that linearity is obtained in this case also<sup>10</sup>.

This result is another illustration of the general property mentioned in the preceding section: here, it is the self-consistent character of the calculation that avoids the IR divergences - the solution automatically adjusts its low  $k$  behavior - and linearity is indeed obtained.

### 2.2.3 Calculation of the linear coefficient $c$

Even when linearity is proved, a difficult problem remains: the calculation of the linear coefficient  $c$ . Analytically, this is an intricate problem, because of its highly non-perturbative character. In the context of non-linear self-consistent equations, we have seen that the problem is non-perturbative at two levels: the choice of the non-linear equation, and the resolution of the equation by successive approximations. In usual perturbation theory, infrared divergences occur in all the integrals contained in the expression of  $\Sigma_{\mathbf{k}}$ , preventing any expansion in the small parameter  $a/\lambda$  around the ideal gas spectrum  $W(\mathbf{k}) = \epsilon_{\mathbf{k}}$ . When one includes higher and higher order in  $a/\lambda$  terms in the energy, these IR divergences become more and more severe, so that higher powers of  $a/\lambda$  in the denominator compensate exactly those in the numerator. As a result, all terms are comparable - see the more detailed discussion of refs. [3, 4], which show that diagrams of all orders in  $a/\lambda$  may contribute comparable amounts to the small momentum part of the spectrum, and therefore to the critical temperature shift. The complexity of the general problem is illustrated by the second leading correction: instead of being proportional to  $a^2$ , as one could naively expect, it is proportional to  $a^2 \log a$ , and therefore manifestly non-analytic [5, 20].

However, if we are only interested in the leading order (linear) shift of  $T_c$ , a simplification is that factors  $[e^{\beta(\epsilon_{\mathbf{k}} - \mu + \Sigma_{\mathbf{k}})} - 1]^{-1}$  can systematically be replaced by  $[\beta(\epsilon_{\mathbf{k}} - \mu + \Sigma_{\mathbf{k}})]^{-1}$ ; in other words, the problem reduces to classical field theory, a case in which the temperature shift is exactly proportional to  $a$  to all orders [4]. This simplification can be regarded as the generalization to all higher order contributions of the approximation of (23) by (24). In the absence of non-linear  $a$  terms, numerical calculations for finite values of  $a$  are in principle easier, since a sometimes delicate extrapolation to zero  $a$  values becomes unnecessary. Nevertheless, in practice, space discretization

<sup>10</sup>In our proof, we have taken for granted the existence of a self-consistent expression for the effective energies, as in Green's function theory. The other assumption is the existence of a solution to the non-linear equation.

introduces another length, the lattice parameter, which may re-introduce non-linearities; a careful extrapolation of the lattice parameter to zero is then necessary. Taking this into account, numerical lattice calculations [14, 15] have indeed provided a precise value,  $c \simeq 1.3$ , which appears to be the best determination to date of this coefficient. On the other hand, classical field theory does not offer an analytic solution, since it is a priori not possible to select a class of well defined perturbation diagrams that are sufficient to give a reasonable value for  $c$ .

Finally, another approach to the problem is given by the “large  $N$ ” expansion, where one studies the critical temperature of a gas containing particles with many internal states, resulting in an order parameter with  $N$  components; the problem is exactly soluble in the limit  $N \rightarrow \infty$  [21] and the calculation of various  $1/N^p$  corrections [21, 22] allows one to extrapolate to the case where the particles have only one internal state ( $N = 2$ ). Other perturbative-variational methods have also been used, see [23, 24, 25, 26, 27, 28].

## 2.3 Discussion

We have already mentioned in § 2.1 that a spatial rearrangement of atoms with low energies takes place, a similar effect to that discussed by Lamb et al. [13], but in the space of the relative positions of the particles (correlations) instead of their ordinary positions. The effect is maximal at  $\mathbf{k} = 0$ , so that the atoms in this level condense more easily than they would in a simple repulsive mean field with no  $\mathbf{k}$  dependence; of course, atoms with very low  $\mathbf{k}$  undergo a similar effect, which vanishes progressively when their momentum increases beyond  $k_c$ . The resulting spectrum  $e_{\mathbf{k}} + \Sigma_{\mathbf{k}}$  is shown schematically in figure 5-a, with the origin of the energies at  $\Sigma_0$  (the value of the chemical potential at transition); for comparison, a purely parabolic spectrum is also shown (dashed line). Figure 5-b shows the corresponding variations of the populations  $\rho_{\mathbf{k}}$ , multiplied by  $k^2$  in order to give directly their contribution to the total population  $N$ . At condensation, when  $\mathbf{k} \rightarrow 0$ , the function goes to a constant for the ideal gas (dashed line), but to zero for the ideal gas (full line) - in the presence of interactions, the delta function corresponding to the presence of a Bose-Einstein condensate appears with no pedestal. The comparison between the situations for the ideal gas and the repulsive gas immediately shows that every  $\mathbf{k} \neq 0$  level is less populated at the critical point in the presence of interactions. Therefore,  $\Delta n_c$  is negative at constant  $T$ , or conversely  $\Delta T_c$  is positive at constant  $n$ <sup>11</sup>.

### 2.3.1 Role of the spectrum

As in [3, 4], we introduce the function  $U(\mathbf{k})$  by:

$$U(\mathbf{k}) = \frac{2m}{\hbar^2} [\Sigma_{\mathbf{k}} - \Sigma_0] = (2\pi\lambda^2)^{-1} [W(\mathbf{k}) - \beta e_{\mathbf{k}}] \quad (31)$$

If we replace in (10)  $\rho_{\mathbf{k}}$  by the long wavelength approximate form  $[\beta(e_{\mathbf{k}} + \Sigma_{\mathbf{k}} - \Sigma_0)]^{-1}$ , we can express the change of the critical density created by the interactions as:

$$\Delta n_c \simeq -\frac{2}{\pi\lambda^2} \int dk \frac{U(k)}{k^2 + U(k)} \quad (32)$$

A priori, one could imagine that the value of  $\Delta n_c$  depends crucially on the details of the spectrum near  $\mathbf{k} = 0$ . Actually, the density change depends mostly on one parameter, the crossover point where  $U(k)$  becomes equal to  $k^2$  (the point at which the energy shift introduced by the interaction equals the kinetic energy); it is relatively insensitive to the details of the variations of the spectrum. For very low values of  $k$  ( $\ll k_c$ ), the role of the function  $U(k)$  is to harden the free particle spectrum so that integrals such as (15) converge; therefore  $U(k) \gg k^2$  and the integrand in (32) is almost unity. For a value  $k_c$  of  $k$  comparable to  $a/\lambda^2$ , see equation (20), there is a crossover between the two functions, and one can expect that one rapidly reaches the opposite regime where  $k^2 \gg U(k)$

<sup>11</sup>Mathematically, a negative value is not totally excluded, but it would require complicated compensation effects and somewhat unpalatable  $k$  variations of  $\Sigma_{\mathbf{k}}$ .

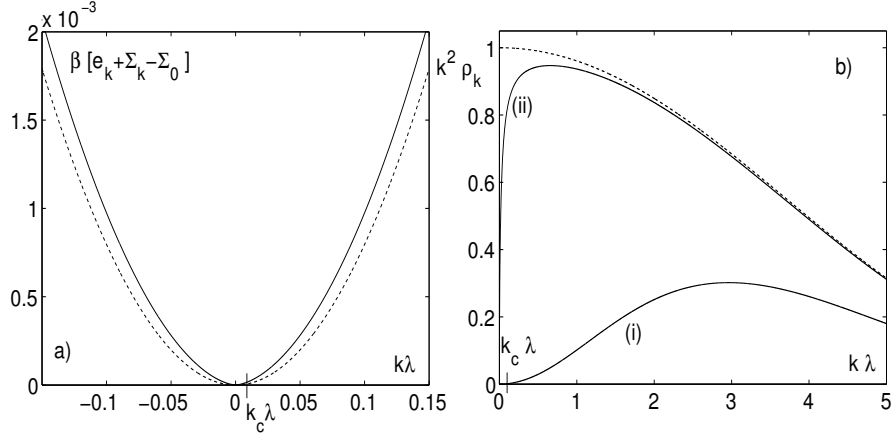


Figure 5: Figure (a): plot of the function  $e_{\mathbf{k}} + \Sigma_{\mathbf{k}}$  (full line), with the origin of the energies at  $\Sigma_0$ , and of the same function for the ideal gas (dashed line). Figure (b) shows the populations  $\rho_{\mathbf{k}}$ , multiplied by  $k^2$ , far above Bose Einstein condensation (curve (i)), and exactly at the condensation point (curve (ii)); again, the ideal gas curve is shown by a dashed line. Because of the modified spectrum, the curve goes to zero at the origin in the presence of repulsive interactions, unlike the ideal gas.

and the integrand in (32) is almost zero. Altogether, we almost find an “all or nothing” regime where the population depletion jumps rapidly from complete to zero, so that:

$$\Delta n_c \simeq -\frac{2}{\pi\lambda^2}k_c \quad (33)$$

which depends only on the value of  $k$  at the crossover and not on the details of the variations of  $U(k)$ . This explains in particular why the calculation of the critical density, or of the critical temperature, is relatively insensitive to the exact value of the universal coefficient  $\eta$  which characterizes the power dependence of  $U(k) \sim k^{2-\eta}$  at low  $k$ .

### 2.3.2 Role of exchange cycles

Feynman has emphasized the role of exchange cycles in Bose-Einstein condensation [29, 30]: condensation takes place when a macroscopic exchange cycle can propagate across the whole sample - see also Elser’s work [31], as well as [32] for a review. The notion of exchange cycles arises in first quantization, where identical particles are numbered, and where a symmetrization operator  $S$  is applied in a second step to obtain the correct physical states. This operator can be decomposed into cycles of particles, usually visualized as a closed path joining all the particles involved [32]. The probability of occurrence of a given path decreases rapidly when the distance between two consecutive particles much exceeds the thermal wavelength  $\lambda$ ; this provides the length scale for the maximum jump of a cycle between particles

Reference [33] discusses how the shift of the critical temperature introduced by the interactions in a homogeneous system can be interpreted in terms of exchange cycles. In an ideal Bose gas just above the transition point, the density fluctuations are large because exchange effects tend to bunch the particles together. There will be regions of space where the density is lower than average and where, because of the maximum length  $\lambda$  of the jump of an exchange path, cycles will not easily propagate; clearly, this effect will oppose the appearance of Bose-Einstein condensation. On the other hand, in a dilute repulsive gas, mutual repulsions create a restoring force which tends to make the system more homogeneous; the occurrence of large regions of low density fluctuations becomes unlikely. This will facilitate the propagation of large exchange cycles across the whole system, i.e.,

Bose-Einstein condensation. Therefore, a lower density (or conversely a higher temperature) are needed to reach condensation<sup>12</sup>.

At this point, one may wonder what is the relation between this physical explanation and the calculations presented above: what is relevant is the effects of IR divergences, and therefore physical properties of the system at very large distances; in this section, what matters is the correlations of particles at a distance of the order of  $\lambda$ . This apparent paradox is removed if one remembers that, in our preceding discussion, we were studying one-body properties; here we are dealing with the propagation of exchange cycles, which depends on two-body properties. A phenomenon which appears at long distances for single particles can translate into shorter range properties for correlations. Here, we will not give a precise discussion of this point, but just develop a plausibility argument. We use a simplified model where the two-body density operator  $\rho_{II}$  in the gas is given by:

$$\rho_{II}(1, 2) = [\rho_I(1) \otimes \rho_I(2)] [1 + P_{\text{ex}}] + \dots \quad (34)$$

where  $\rho_I$  is the one-body density operator and  $P_{\text{ex}}$  is the exchange operator between particles 1 and 2. This relation is exact for the ideal gas, but only an approximation for the interacting gas. Even if some effects of the interactions are already contained in (34) through changes of the  $\rho_I$ 's, it is clear that more terms should be added to the right of (34) to get an exact formula - in particular terms that introduce short range correlations between the particles. This approximation is sufficient for our present qualitative discussion.

The direct term in the right side of (34) is simply a product containing no spatial correlation, so that we will ignore it and focus on the exchange term containing  $P_{\text{ex}}$  with diagonal elements:

$$\langle \mathbf{r}_1, \mathbf{r}_2 | \rho_{II}^{\text{ex}}(1, 2) | \mathbf{r}_1, \mathbf{r}_2 \rangle = \langle \mathbf{r}_1, \mathbf{r}_2 | \rho_I(1) \otimes \rho_I(2) | \mathbf{r}_2, \mathbf{r}_1 \rangle \quad (35)$$

Since one-particle density operators are diagonal in the momentum representation (translational invariance), this term is proportional to:

$$\int d^3 k_1 \int d^3 k_2 \rho_{\mathbf{k}_1} \rho_{\mathbf{k}_2} e^{i(\mathbf{k}_1 - \mathbf{k}_2) \cdot (\mathbf{r}_1 - \mathbf{r}_2)} \quad (36)$$

Therefore the two-body correlation function is independent of the sum  $\mathbf{r}_1 + \mathbf{r}_2$  (position of the center of mass of the two particles), while its  $\mathbf{r}_1 - \mathbf{r}_2 = \mathbf{r}$  dependence is given by the Fourier transform of the integral:

$$\int d^3 K \rho_{(\mathbf{K}+\mathbf{k})/2} \times \rho_{(\mathbf{K}-\mathbf{k})/2} \quad (37)$$

which, using parity, can be expressed as a convolution integral:

$$\int d^3 K \rho_{(\mathbf{k}+\mathbf{K})/2} \times \rho_{(\mathbf{k}-\mathbf{K})/2} \quad (38)$$

At the critical point, we have seen above that the distribution function  $\rho_{\mathbf{k}}$  is the sum of two components: a Bose-Einstein distribution obtained within a mean-field approximation with a slightly negative value of the effective chemical potential (proportional to the square of the scattering length  $a$ ), and a critical perturbation introduced for small  $k$  (comparable to  $k_c$ ) by the correlation effects; the latter is difficult to calculate, but small. We therefore have:

$$\rho_{\mathbf{k}} = \rho_{\mathbf{k}}^{(0)} + \Delta\rho_{\mathbf{k}} \quad (39)$$

where the first term has a width comparable to  $1/\lambda$  while the second has a width  $k_c$ . The two-body correlation function now appears as the sum of three terms: a term in  $[\rho_{\mathbf{k}}^{(0)}]^2$ , a crossed term in

---

<sup>12</sup>This is actually an interesting situation: in most cases, repulsive interactions between particles tend to mask quantum effects, especially exchange effects (for instance, hard core potential effects reduce exchange effects in liquid helium three and four); for the dilute system here, they actually enhance them.

$\rho_{\mathbf{k}}^{(0)} \times \Delta\rho_{\mathbf{k}}$  on which we will focus our interest, and finally a term in  $[\Delta\rho_{\mathbf{k}}]^2$ , which we will ignore since it is smaller.

The first term is well-known [34]: it corresponds essentially to an ideal Bose gas close to the transition point and contains the usual “exchange bump”, with a width comparable to  $\lambda$ , as well as a long exponential tail<sup>13</sup>. The second term is the crossed term; its Fourier transform appears as the convolution of the function  $\rho_{\mathbf{k}/2}^{(0)}$  by  $\Delta\rho_{\mathbf{k}/2}$ . Since  $\Delta\rho_{\mathbf{k}/2}$  is much narrower than  $\rho_{\mathbf{k}/2}^{(0)}$ , the function  $\Delta\rho_{\mathbf{k}/2}$  may be approximated by a delta function at the origin, with a positive weight  $d$ . We then obtain for the Fourier transform of this term:

$$d \times \rho_{\mathbf{k}/2} \quad (40)$$

This corresponds to a change of the spatial correlation function that is positive; it has basically the same spatial dependence as the zero order term, except that no squared function appears here. It therefore contains an exchange bump that extends to distances comparable to the thermal wavelength, but slightly further because it no longer includes a convolution of two  $\rho$ 's; there still is a long exponential tail, with twice the range of the zero order tail.

This simple model illustrates how the physics behind the reduction of the critical density may appear at a different scale, depending whether it is expressed in terms of single particle properties or in terms of correlations. In the former case, the critical phenomenon is contained in  $\Delta\rho_{\mathbf{k}}$ , which contains mostly small  $\mathbf{k}$ 's and is dominated by long distances; in the latter,  $\Delta\rho_{\mathbf{k}}$  disappears from the leading term, so that distances of the order of  $\lambda$  remain relevant.

### 3 Mean field and correlation effects combined in a trap

As already mentioned, in the thermodynamic limit, Bose-Einstein condensation is reached in a trap when the density at the center of the trap is exactly the critical density for a uniform gas, including of course the corrections introduced by the correlations. Two effects (the compressibility effect of § 1 and the correlation effect of § 2) then add to each other<sup>14</sup> to determine the change of the critical value of  $N$  at a given temperature (or, conversely, the critical temperature at fixed  $N$ ). Nevertheless, as remarked by Arnold and Tomasik [35], their combination is not trivial because spatial effects in a trap mix up various orders in  $a$ . In this section we study the effects of the interactions on the density profile of a gas in a trap, assuming that the temperature is above, or just at the critical temperature. We start from the number density at the center, from which we can calculate the density profile by using an equation of state obtained within mean field approximation. The critical density profile is then derived by setting the density at the center to its critical value, including the correlation effects discussed in the preceding sections, which are beyond mean field theory. There is nevertheless no inconsistency in this approach; the reason is that the calculation of the equation of state of the gas reduces to an ordinary virial correction to the pressure, which is perturbative, while the calculation of the critical density remains essentially non perturbative.

We will see that the specific properties of the curves of figure 1 play a role in this problem, in particular the large compressibility of the gas at the critical point. Roughly speaking, the compressibility of the gas at the center of the trap is large ( $\sim 1/a$ ), but remains much smaller in most other regions of the trap (practically independent of  $a$ ). One can then anticipate that a change of the pressure that is only second order in  $a$  will correspond to a change of the density of the same order in those regions, but first order at the center. This will allow one to meet the change of the condensation condition introduced by the correlations effects. But, since  $N$  is primarily determined by the density of the gas in those low compressibility regions, this change corresponds to a second order variation<sup>15</sup> of  $N$ . We now discuss this question more precisely.

<sup>13</sup>The tail can easily be obtained by using the approximation  $\rho_{\mathbf{k}}^{(0)} \sim \beta^{-1}(e_{\mathbf{k}} - \mu)^{-1}$ , equivalent to a zero Matsubara frequency approximation - see for instance exercise 12.9 of [1]. Since the effective chemical potential is proportional to  $a^2$  at the transition point, the range of this exponential tail is of order  $\lambda^2/a$ .

<sup>14</sup>More precisely, subtract from each other, since they have opposite signs.

<sup>15</sup>Conversely, one can assume that  $N$  is fixed and that the temperature is reduced from above the transition; the



### 3.1 Density profile

In a first step, we consider the number density of the gas at the center of the trap  $n(0)$  as a free parameter. We come back to equation (7) and distinguish two cases:

(i) Classical gas ( $n\lambda^3 \ll 1$ )

The relation between the chemical potential and the density is then  $\beta\mu_{\text{eff}} \simeq \ln(n\lambda^3)$ , which implies  $J' \simeq 1/n\lambda^3$ , so that (7) becomes:

$$-\nabla [\beta V + 4a\lambda^2 n] = \nabla \ln(n) \quad (41)$$

An  $\mathbf{r}$  integration then gives:

$$n \sim \exp [-\beta V - 4a\lambda^2 n] \quad (42)$$

which is nothing but the usual Boltzmann exponential. Around the center of the trap, the density varies proportionally to the potential energy  $V$ :

$$n(\mathbf{r}) \simeq n(0) \left[ 1 - \frac{\beta V(\mathbf{r})}{1 + 4a\lambda^2 n(0)} + \dots \right] \quad (\text{if } r \rightarrow 0) \quad (43)$$

(ii) Quantum non condensed gas ( $1 \lesssim n\lambda^3 \leq \zeta_{3/2}$ )

For simplicity, we assume that the gas is strongly degenerate at the center of the trap ( $n(0)\lambda^3$  is close to  $\zeta_{3/2}$ ), and we limit our study to the region of the trap where this degeneracy remains strong. We can then use the Mellin formula limited to lowest order (a more precise calculation is given in the appendix):  $g_{3/2}(\exp \beta\mu) \simeq \zeta_{3/2} - 2\sqrt{-\pi\beta\mu}$  [2, 37], where  $\zeta_{3/2}$  is the value at the origin of the  $g_{3/2}$  function ( $\zeta_{3/2} = g_{3/2}(z = 1) \simeq 2.61\dots$ ). This provides:

$$J \simeq -\frac{1}{4\pi} (n\lambda^3 - n_c^0\lambda^3)^2 + \dots \quad (44)$$

where:

$$n_c^0 = \zeta_{3/2} \lambda^{-3} \quad (45)$$

is the critical density of the ideal gas. This result, inserted into (7), allows us to integrate the gradients on each side of the equation and yields (assuming that the potential at the center of the trap vanishes):

$$-\beta V = -\frac{\lambda^6}{4\pi} \left[ (n - n_c^0)^2 - (n(0) - n_c^0)^2 \right] + 4\frac{a}{\lambda} (n - n(0)) \lambda^3 \quad (46)$$

This equation is second degree in  $n$ ; choosing the solution which tends to  $n(0)$  when  $r \rightarrow 0$  provides:

$$n(\mathbf{r}) = n_c^0 + \frac{8\pi a}{\lambda^4} - \sqrt{\left[ n_c^0 - n(0) + \frac{8\pi a}{\lambda^4} \right]^2 + \frac{4\pi}{\lambda^6} \beta V(\mathbf{r})} \quad (47)$$

Equation (47) gives the density profile of the gas as a function of  $\mathbf{r}$ , provided that the gas is in the quantum regime.

For an ideal gas ( $a = 0$ ), figure 6-a shows the density profiles obtained as a function of the central density  $n(0)$ , assuming a quadratic potential  $V(\mathbf{r}) \sim r^2$ ; as usual, the thermal range  $R_T$  is defined<sup>16</sup> by  $(r/R_T)^2 = \beta V(r)$ . If  $n(0) = n_c^0$ , the density variations are linear in  $r$  in all the quantum region; for lower values of  $n(0)$ , there is a parabolic variation near the center of the trap, in a domain that becomes larger and larger when  $n_c^0 - n(0)$  increases.

For an interacting gas ( $a > 0$ ), one can distinguish in (47) two possibilities, depending whether the potential energy  $\beta V$  is larger or smaller than  $[(n_c^0 - n(0)) \lambda^3 + 8\pi a/\lambda]^2$ . Near the center of size of the atomic cloud then decreases progressively. When the system reaches a temperature close to condensation, the compressibility at the center becomes  $\sim 1/a$  and therefore very large, so that particles tend to accumulate more around this point of space than elsewhere in the trap. Consequently, a second order in  $a$  change of the temperature is sufficient to create a first order change of the local density.

<sup>16</sup> $R_T$  is the size of the ideal classical gas in the trap at temperature  $T$ .

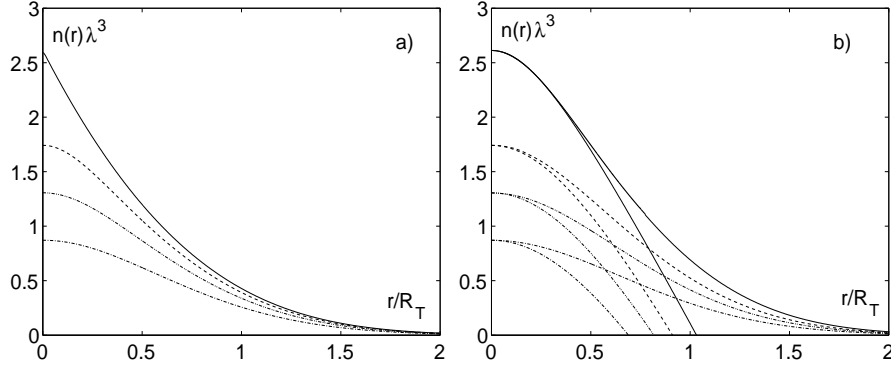


Figure 6: Figure (a) shows the modification of the density profile for the trapped ideal gas when increasing the central density until it reaches the condensation condition (full line:  $n(0)\lambda^3 = \zeta_{3/2}$ ; dashed line:  $n(0)\lambda^3 = 2\zeta_{3/2}/3$ ; dash-double dot line:  $n(0)\lambda^3 = \zeta_{3/2}/2$ ; dash-dot line:  $n(0)\lambda^3 = \zeta_{3/2}/3$ ). Figure (b) shows the corresponding density profile for the trapped repulsive gas calculated within mean field theory. The asymptotes at the center of the trap are calculated with the lowest order approximation of the Mellin formula, equation (47).

the trap,  $V$  is small and the density variation is proportional to  $V$  (quadratic in  $\mathbf{r}$  for a harmonic potential):

$$n(\mathbf{r}) \simeq n(0) - \frac{2\pi\beta V(\mathbf{r})}{\lambda^3 [(n_c^0 - n(0))\lambda^3 + (8\pi a/\lambda)]} + \dots \text{ (if } r \rightarrow 0 \text{)} \quad (48)$$

This formula is similar to (43) but predicts significantly different results. For instance, if  $a$  is sufficiently small and if the central density is sufficiently close to its critical value, the change of the density induced by the potential becomes arbitrarily large - while it remains constant for a classical gas; this is a consequence of the large compressibility of the quantum gas at the origin. Further from the center of the trap,  $V$  is large, and (47) becomes:

$$n(\mathbf{r}) \simeq n_c^0 + \frac{8\pi a}{\lambda^4} - \sqrt{\frac{4\pi\beta V(\mathbf{r})}{\lambda^6}} \left[ 1 + \frac{[(n_c^0 - n(0))\lambda^3 + (8\pi a/\lambda)]^2}{8\pi\beta V(\mathbf{r})} + \dots \right] \quad (49)$$

which now predicts a square root dependence in  $V$ . Figure 6-b illustrates these two different behaviors of the density.

### 3.2 Critical density profile

We are now in position to discuss the effects of the interactions on the density profile at the transition point, at least in the central region of the trap where the gas remains strongly degenerate. We set the central density to its critical value  $n_c$  and use the above equations to calculate  $n(\mathbf{r})$ . This calculation is of course not exact, for different reasons: first, (47) is only valid within mean field theory; second, the use of the first correction only in the Mellin formula limits us to a sufficiently degenerate gas. Both approximations could be improved: the first by including second order perturbative corrections to the equation of state, as done in ref. [35]; the second by including more terms in the Mellin formula, as done in the appendix. Our calculation nevertheless remains sufficient for a qualitative discussion.

Let us first ignore the effects of the correlations on the critical density at the center. We then set  $n(0) = n_c^0$  and see that the density corrections are positive and first order in  $a$  everywhere in the trap - second term in the right side of eq. (49) - except in a small region around the center where the density change is still positive but  $\propto 1/a$  - fraction in the right side of eq. (48). For a harmonic potential, this small region has a size proportional to  $a$ , so that the corresponding

contribution to  $N$  is only second order in  $a$ . Therefore, the main contribution arises from all the rest of the trap and provides a first order in  $a$  change of  $N$  (at constant temperature); conversely, calculating the temperature shift at constant  $N$  provides (8), as shown in ref. [8].

We now take into account the effects of the correlations on the critical density at the center of the trap. We then need to choose a slightly smaller value of  $n(0)$  since, according to (26),  $n_c$  is reduced by an amount that is first order in  $a$ . With respect to the calculation of the preceding paragraph, eq. (48) predicts an additional negative change, first order in  $a$ , of the density around the center of the trap. On the other hand, eq. (49) predicts only a second order change induced by the new value of  $n(0)$ ; the crossover between the regions of space where these equations apply is obtained when the potential energy is second order in  $a$ , i.e., at a first order distance from the origin if the potential is harmonic. This corresponds only to a fourth order correction to the total number of particles  $N$ , because the volume of this region is proportional to  $a^3$  for a harmonic potential; this correction remains therefore negligible when compared to the second order in  $a$  contribution from all other regions in the trap. Altogether, we see that the additional change of  $N$  introduced by the correlation effects is therefore only second order in  $a$ ; this is to be compared with the first order correction introduced by mean field effects contained in the term in  $a/\pi\lambda^4$  on the right side of (47).

We therefore recover the conclusions of Arnold and Tomasik [35]: the two  $N$  changes subtract from each other, but not at the same order in  $a$ . This offset of one order illustrates again the relatively loose connection between the total number of atoms in the trap  $N$  and the physics at the center, where Bose-Einstein first takes place: most of the particles contributing to  $N$  are too far from condensation to play a role in it. If the central density  $n(0)$  were accessible, it would provide a more adequate variable than  $N$  for the study of the BEC phenomenon. See ref. [36] for a proposal of a method (adiabatic ramping down of the trap frequency) aimed at enhancing the visibility of the correlation effects against the background of mean field effects.

## 4 Conclusion

The calculation of the critical temperature of a dilute Bose gas has several distinguishing features. One could of course try to go further than the leading  $a$  correction to the critical temperature and attempt to describe analytically the full density variations obtained by path integral Monte Carlo methods in [33]. Quantitatively it is clear that at high densities the blocking of exchange created by the repulsive hard core part of the potential tends to reduce the critical temperature, an effect which goes in the opposite direction to what happens for dilute gases. Ref. [38] gives a discussion of this effect in terms of change of the effective mass of the particles, arising from a  $k$  dependence of the exchange term in the expression of the mean field. It would be interesting to make this idea more quantitative and to explore the specific details of BEC in all density regimes.

ACKNOWLEDGMENTS: We gratefully thank Peter Arnold and Masud Haque for several useful discussions. Laboratoire Kastler Brossel is “laboratoire associé ENS-CNRS-UPMC UMR 8552”. Laboratoire de Physique Théorique des Liquides is “laboratoire associé du CNRS et de l’UPMC Paris 6, UMR 7600”. One of the authors (J.N.F.) is grateful to “Association Dephy” for a research grant and to “Société Française de Physique” for its support. This research was supported in part by US National Science Foundation Grant PHY00-98353.

## APPENDIX

A better approximation for  $g_{3/2}$  than that used in § 3 is:

$$g_{3/2}(\exp \beta\mu) \simeq \zeta_{3/2} - 2\sqrt{-\pi\beta\mu} - b \beta\mu + \dots \quad (50)$$

with  $b = 1.46..$  [2, 37]. Adding a linear term to the square root actually provides values which are reasonably accurate until  $\beta\mu$  reaches values where the classical regime is obtained ( $\beta\mu < -1$ ).

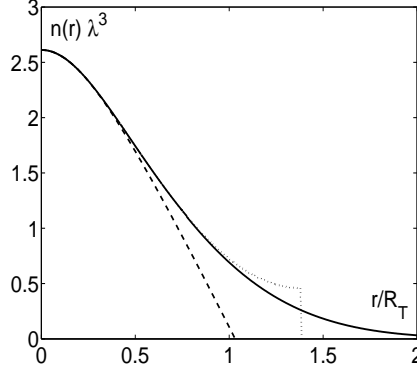


Figure 7: Full line: mean field density profile calculated exactly (equation (4)). Dashed line: same profile with the lowest order approximation of the Mellin formula (equation (47)). Dotted line: same profile with the inclusion of the linear correction (equation (53)).

Inverting the relation  $n\lambda^3 = g_{3/2}(\exp \beta\mu_{\text{eff}})$  then gives:

$$-\beta\mu_{\text{eff}} = \frac{\pi}{b^2} \left[ 2 + \frac{b}{\pi} (n - n_c^0) \lambda^3 - 2\sqrt{1 + \frac{b}{\pi} (n - n_c^0) \lambda^3} \right] \quad (51)$$

which defines the function  $J(n\lambda^3)$ . We therefore have:

$$J' = -\frac{1}{b} \left[ 1 - \frac{1}{\sqrt{1 + b\lambda^3 (n - n_c^0) / \pi}} \right] \quad (52)$$

Relation (7) then becomes, after integration of the gradients:

$$-\beta V = 4a\lambda^2 (n - n(0)) - \frac{\lambda^3}{b} \left[ (n - n(0)) - \frac{2\pi}{b\lambda^3} \sqrt{1 + b\lambda^3 (n - n_c^0) / \pi} + \frac{2\pi}{b\lambda^3} \sqrt{1 + b\lambda^3 (n(0) - n_c^0) / \pi} \right] \quad (53)$$

This equation provides a direct relation between the potential energy and the local density. For instance, for a quadratic potential, the position  $r$  is obtained by taking the square root of the right side, multiplied by some coefficient. This allows one to make a precise calculation of the density profile in all regions of the trap where the gas is in a quantum regime. Figure 7 gives a comparison between the density profile obtained in the mean field approximation with (53) and (47).

## References

- [1] K. Huang, “Statistical Mechanics”, Wiley (1963).
- [2] R.K. Pathria, “Statistical Mechanics”, Pergamon Press (1972).
- [3] G. Baym, J-P. Blaizot, M. Holzmann, F. Laloë and D. Vautherin, Eur. Phys. J. **B 24**, 107 (2001).
- [4] G. Baym, J-P. Blaizot, M. Holzmann, F. Laloë and D. Vautherin, Phys. Rev. Lett. **83**, 1703 (1999).
- [5] M. Holzmann, G. Baym, J-P. Blaizot and F. Laloë, Phys. Rev. Lett. **87**, 120403 (2001).
- [6] F. Dalfovo, S. Giorgini, L.P. Pitaevskii, S. Stringari, Rev. Mod. Phys. **71**, 463 (1999).

- [7] M. Holzmann, P. Grüter and F. Laloë, Eur. Phys. J. **B10**, 739 (1999).
- [8] S. Giorgini, L. Pitaevskii and S. Stringari, Phys. Rev. **A54**, 4633 (1996).
- [9] F. Gerbier, J.H. Thywissen, S. Richard, M. Hugbart, P. Bouyer and A. Aspect, cond-mat/0307188.
- [10] W. Krauth, Phys. Rev. Lett. **77**, 3695 (1996).
- [11] M. Holzmann, W. Krauth and M. Naraschewski, Phys. Rev. **A59**, 2956 (1999).
- [12] J.N. Fuchs, M. Holzmann and F. Laloë, Eur. Phys. J. **B25**, 463 (2002).
- [13] W.E. Lamb and A. Nordsieck, Phys. Rev. **15**, 677 (1941).
- [14] P. Arnold and G. Moore, Phys. Rev. Lett. **87**, 120401 (2001).
- [15] V.A. Kashurnikov, N.V. Prokof'ev and B. Svistunov, Phys. Rev. Lett. **87**, 120402 (2001).
- [16] M. Bijlsma and H.T.C. Stoof, Phys. Rev. **A54**, 5085 (1996); see in particular §IVB and fig. 6.
- [17] A.Z. Patashinskii and V.L. Pokrovskii, Zh. E.T.F. **46**, 994 (1964); Sov. Phys. JETP **19**, 677 (1964).
- [18] M. Haque and A. Ruckenstein, cond-mat/02125590.
- [19] H.T.C. Stoof, Phys. Rev. **A45**, 8398 (1992).
- [20] P. Arnold, G. Moore and B. Tomasik, Phys. Rev. **A65**, 013606 (2001).
- [21] G. Baym, J-P. Blaizot and J. Zinn-Justin, Eur. Phys. Lett. **49**, 150 (2000).
- [22] P. Arnold and B. Tomasik, Phys. Rev. **A62**, 063604 (2000).
- [23] F.F. de Souza Cruz, M.B. Pinto and R.O. Ramos, Phys. Rev. **B64**, 014515 (2001).
- [24] F.F. de Souza Cruz, M.B. Pinto, R.O. Ramos and P. Sena, Phys. Rev. **A65**, 053613 (2002).
- [25] E. Braaten and E. Radescu, cond-mat/0206186.
- [26] H. Kleinert, cond-mat/0210162.
- [27] B. Kastening, cond-mat/0303486.
- [28] B. Kastening, cond-mat/0309060.
- [29] R.P. Feynman, Phys. Rev. **91**, 1291 (1953).
- [30] R.P. Feynman, "Statistical Mechanics, a set of lectures", Benjamin (1972).
- [31] V. Elser, "The loop gas picture of the lambda transition", from "Topics in Statistical mechanics", PhD thesis, 1984.
- [32] D.M. Ceperley, Rev. Mod. Phys. **67**, 279 (1995).
- [33] P. Grüter, D. Ceperley and F. Laloë, Phys. Rev. Lett. **79**, 3549 (1997).
- [34] L. Van Hove, Phys. Rev. **95**, 249 (1954).
- [35] P. Arnold and B. Tomasik, Phys. Rev. **A64**, 053609 (2001).
- [36] M. Houbiers, H.T.C. Stoof and E.A. Cornell, Phys. Rev. **A56**, 2041 (1997).
- [37] J.E. Robinson, Phys. Rev. **83**, 678 (1951).
- [38] A.L. Fetter and J.D. Walecka, "Quantum theory of many particle systems", Mc Graw Hill (1971); see §28.